Investigation of hindwing folding in ladybird beetles by artificial elytron transplantation and microcomputed tomography

Kazuya Saito[a,1], Shuhei Nomura[b], Shuhei Yamamoto[c], Ryuma Niyama[d], and Yoji Okabe[a]

[a]Institute of Industrial Science, The University of Tokyo, 4-6-1 Komaba, Tokyo, 153-8505 Japan; [b]National Museum of Nature and Science, 4-1-1 Amakubo, Tsukuba-shi, Ibaraki 305-0005 Japan; [c]Graduate School of Bioresource and Bioenvironmental Sciences, Kyushu University, 6-10-1 Hakozaki, Fukuoka, 812-8581 Japan; and [d]Graduate School of Information Science and Technology, The University of Tokyo, 7-3-1 Hongo, Tokyo, 113-8654 Japan

Edited by David A. Weitz, Harvard University, Cambridge, MA, and approved April 17, 2017 (received for review December 20, 2016)

Ladybird beetles are high-mobility insects and explore broad areas by switching between walking and flying. Their excellent wing transformation systems enabling this lifestyle are expected to provide large potential for engineering applications. However, the mechanism behind the folding of their hindwings remains unclear. The reason is that ladybird beetles close the elytra ahead of wing folding, preventing the observation of detailed processes occurring under the elytra. In the present study, artificial transparent elytra were transplanted on living ladybird beetles, thereby enabling us to observe the detailed wing-folding processes. The result revealed that in addition to the abdominal movements mentioned in previous studies, the edge and ventral surface of the elytra, as well as characteristic shaped veins, play important roles in wing folding. The structures of the wing frames enabling this folding process and detailed 3D shape of the hindwing were investigated using microcomputed tomography. The results showed that the tape spring-like elastic frame plays an important role in the wing transformation mechanism. Compared with other beetles, hindwings in ladybird beetles are characterized by two seemingly incompatible properties: (*i*) the wing rigidity with relatively thick veins and (*ii*) the compactness in stored shapes with complex crease patterns. The detailed wing-folding process revealed in this study is expected to facilitate understanding of the naturally optimized system in this excellent deployable structure.

aerospace engineering | biomimetics | *Coccinella* | Coleoptera | deployable structure

Ladybird beetles are high-mobility insects and explore broad areas by switching between walking and flying. This lifestyle is achieved by an excellent wing transformation system that enables smooth switching between the walking and flight forms. The hindwing deployment in the takeoff motion is very fast and completed within 0.1 s from the fully folded state (Movie S1). Researchers have found that the intrinsic elasticity acting in wing veins allows this high-speed wing deployment (1–6). Investigation in other species of beetles indicated the existence of a hydraulic mechanism that straightens the wing veins (7). In contrast, the other fundamental problem, namely, the mechanism behind the folding of these wings, remains unclear. It can be assumed that wing folding is more difficult than unfolding in ladybird beetles because the wing elasticity, which assists in rapid deployment, would interfere in the folding process of the wings. Nevertheless, ladybird beetles can achieve highly compact wing storage with complex crease patterns. The up-and-down movements in the abdomen are estimated to play an important role in the folding process (2–4); however, how these simple movements can accomplish a complex folded shape remains unclear. Complicating matters further is the fact that ladybird beetles close the elytra ahead of wing folding, preventing the observation of detailed folding processes. In addition, the elytra are required elements for wing folding, and therefore cannot be removed for observations. Wing transformations were described using crease patterns (ground plans) in previous studies (1, 8); however, the actual 3D structures in folded and unfolded wings remain unclear.

To clarify these unknown mechanisms and structures, we first transplanted artificial transparent elytra on living ladybird beetles and observed their wing-folding movements using high-speed cameras. This method revealed the detailed wing-folding mechanism occurring under the elytra. Next, we investigated the bending points in the anterior margin of the hindwing using microcomputed tomography (micro-CT). This part is the most rigid area of the hindwings and is considered to confer the rigidity and strength required for flight. Therefore, a detailed investigation of this area is important for understanding the wing transformation mechanism facilitating compatibility between the deformability required for wing folding and strength property required for flying. The folded hindwings were also investigated by micro-CT, and the actual 3D shape and positional relationship between fold lines and frames were revealed.

Results

The specimens used were *Coccinella septempunctata* (L.), from which two-thirds of the apical right elytron was removed. To reestablish the function of wing folding and to reveal in detail the folding processes, including the midfolded shapes of the hindwings, we transplanted the acrylic transparent elytron. The artificial elytra used were composed of UV light-cured resin constructed using a silicon impression of the undersurface of the removed elytron and transplanted into the original living ladybird beetle. Fig. S1 shows the schematic representation of the transplant

Significance

Hindwings in ladybird beetles successfully achieve compatibility between the deformability (instability) required for wing folding and strength property (stability) required for flying. This study demonstrates how ladybird beetles address these two conflicting requirements by an unprecedented technique using artificial wings. Our results, which clarify the detailed wing-folding process and reveal the supporting structures, provide indispensable initial knowledge for revealing this naturally evolved optimization system. Investigating the characteristics in the venations and crease patterns revealed in this study could provide an innovative designing method, enabling the integration of structural stability and deformability, and thus could have a considerable impact on engineering science.

Author contributions: K.S. and Y.O. designed research; K.S. performed research; K.S., S.N., and R.N. contributed new reagents/analytic tools; K.S., S.N., S.Y., R.N., and Y.O. analyzed data; and K.S. and S.Y. wrote the paper.

The authors declare no conflict of interest.

This article is a PNAS Direct Submission.

Freely available online through the PNAS open access option.

[1]To whom correspondence should be addressed. Email: saito-k@iis.u-tokyo.ac.jp.

This article contains supporting information online at www.pnas.org/lookup/suppl/doi:10.1073/pnas.1620612114/-/DCSupplemental.

operation. The detailed method is explained in *Materials and Methods*. Fig. 1*A* shows the hindwing of *C. septempunctata*. The wing basal component is supported by two thick veins: the mediocubital loop (MCL) and radiomedial loop (RML) (8, 9). The positions of the folding lines in the rest position are shown in Fig. 1*B*. The crease lines can be classified into three types on the basis of their functions. Red lines are the principal transverse fold (PTF) and apical transverse fold (ATF), which fold a wing along the longitudinal direction. Blue lines emerge between the MCL and RML, and fold a wing along the transverse direction. These two types of lines are connected by diamond-shaped crease patterns (green lines). The detailed wing-folding processes are explained with reference to Fig. 1 *C*–*G*. After landing, the elytra are first closed before the hindwing folding commences (Fig. 1*C*). The hindwings are simultaneously aligned backward and protrude out from the closed elytra. Held by the elytron, the wing is slightly folded in the transverse direction (Fig. 1*D*). Then, the ladybird beetle lifts its abdomen, and the hindwings are pressed into the undersurface of the elytron. During this process, the characteristic shape of the MCL fits the curve of the ventral surface of the elytron and ark-like mountain folding lines appear beneath the MCL (Fig. 1*E*). The abdominal lifting movements are observed multiple times. These movements result in the rubbing of the underside of the hindwings and pulling them into the dorsal

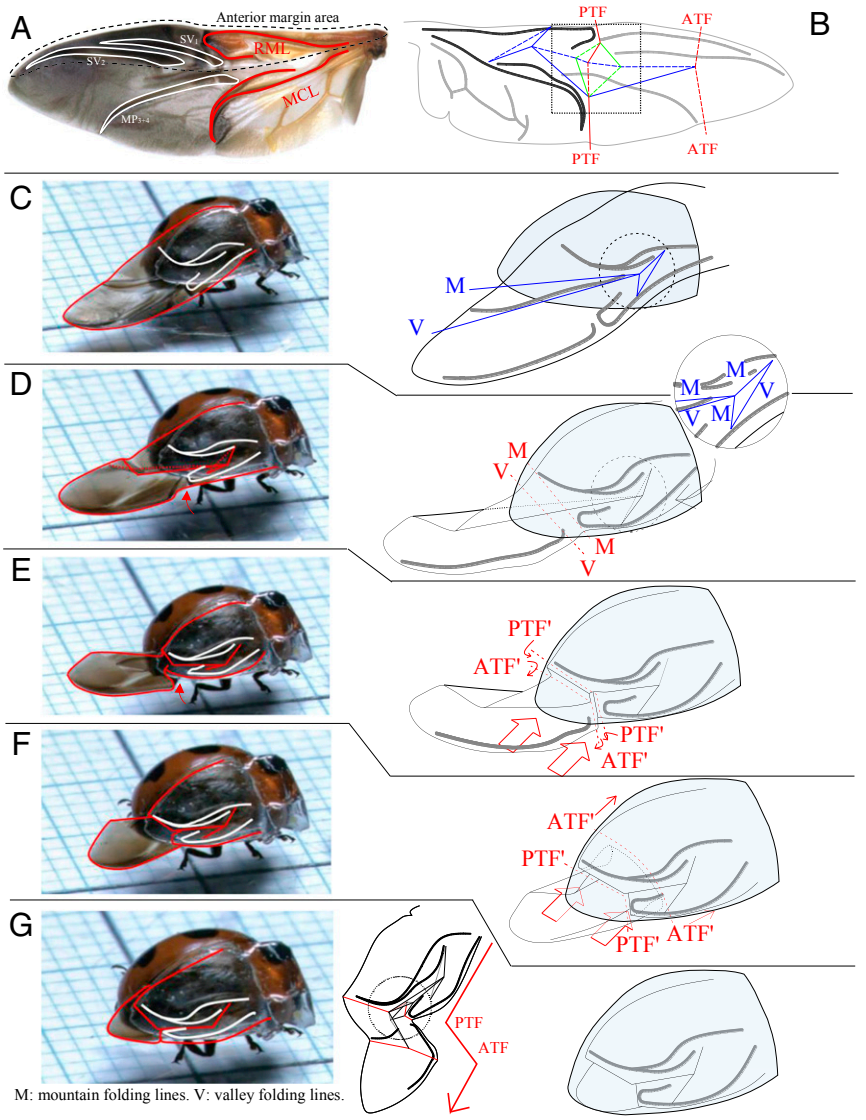

Fig. 1. Wing-folding process in a ladybird beetle. (*A*) Hindwing of *C. septempunctata*. The basal part of the wing is supported by thick two veins: the MCL and RML. (*B*) Main crease lines of hindwing folding. The crease lines can be classified into three types based on their functions. Red lines are the PTF and ATF, which fold the wing along the longitudinal direction. Blue lines emerge between the MCL and RML and fold the wing along the transverse direction. The movements of these two types of lines are connected by diamond-shaped crease patterns (green lines). Fine lines represent mountain folding lines, and dashed lines represent valley folding lines. The dashed-line square corresponds to the paper model of Fig. 3. (*C*–*G*) Schematic representations of the wing-folding process. (*C*) Elytra are closed ahead of the hindwings, and they are simultaneously aligned backward. (*D*) Held by the elytron, the wing is slightly folded in the transverse direction and a triangular crease pattern emerges between the MCL and RML. (*E*) PTF and ATF are first introduced by the inner curve of the elytron and the edge of the elytron with the abdomen (PTF′ and ATF′). (*F*) According to the wing retraction by abdominal movement, the ATF′ drifts toward the apex of the wing by abdominal push and the wing is gradually retracted. The position of the PTF′ is held by the edge of the elytron. Finally, two transverse folding lines are stabilized into the positions of the PTF and ATF as shown in *B*. (*G*) Explanation of the stored shape. The hindwings are folded into a Z-shape on the folding lines of the PTF and ATF, and the diamond-shaped crease pattern emerges in the center of the hindwing.

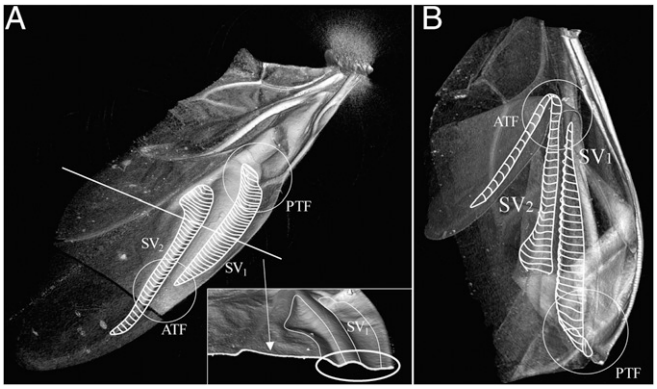

Fig. 2. Three-dimensional models of the hindwings in *C. septempunctata* reconstructed from the results of micro-CT. (*A*, *Upper Left*) Unfolded hindwing (from the underside). (*A*, *Lower Right*) Slice view on the white line is shown. Compared with other parts, the cross-sections of the main supporting veins (SV_1, SV_2) have no difference in thickness but have a characteristic curved shape. (*B*) Folded hindwing. The main supporting veins are bent into a cylindrical shape (white circles) similar to the shape of a tape spring.

storage space. For maximum effectiveness of these movements, the tergal plates contain microspicule patches (*Assisting Structures for Wing Folding* and Fig. S2), which are considered to hold the surface of the hindwings and assist smooth wing folding (2–4). The PTF is introduced by the inner curve of the elytron (PTF′ in Fig. 1*G*) and appears at almost the same position as in Fig. 1*B*. The ATF is initially introduced by the edge of the elytron at the position shown as ATF′ in Fig. 1*E* and gradually drifts toward the apex of the wing guided by the abdominal movements (Fig. 1*F*). Finally, two transverse folding lines (red lines) are stabilized into the positions of the PTF and ATF in Fig. 1*B*, and the diamond-shaped crease pattern (green lines) emerges in the center of the wing. In the stored shape, the hindwings are folded into a Z-shape on the folding lines of the PTF and ATF as shown in in Fig. 1*G* (*Center*). The wing folding is completed within 2.0 s. For better understanding, a high-speed movie of these folding processes is available in Movie S2.

The majority of the hindwing comprises relatively soft membrane. During flights, the hindwing shape is maintained by thick veins. Among them, the anterior margin area (Fig. 1*A*) including the supporting vein 1 (SV_1) and SV_2 veins and the RML, is hard and considered to confer stiffness and strength to the hindwings. We investigated the deformation of this part in both folded and unfolded states using micro-CT. Fig. 2*A* shows the 3D shape of the unfolded wing reconstructed by the result of the CT scan. The thicknesses of these main veins have no difference from other areas; however, their cross-sections have a characteristic curved shape similar to the shape of a tape spring (10–13). No special structures, including articulations, thinner parts, or an inner cavity, are observed on the cross-point of the crease lines and veins. Fig. 2*B* shows the 3D model of the folded hindwing. It is observed that the anterior margin is bent into a cylinder shape with a constant curvature instead of being bent at a sharp angle (white circles in Fig. 2). The bent shapes of these veins are similar to the shapes of the localized folds (10) observed in a tape spring. For better understanding of the shape of the folded wing, a translucent 3D image is available in Movie S3.

Discussion

With respect to the wing venation, two loop-shaped veins (MCL and RML) are a common feature found in many beetle species; however, the MCLs in ladybird beetles have characteristic arc-like shapes. As mentioned above, this shape functions to introduce the crease lines by fitting the ventral curve of the elytron. These steady venations not only confer sufficient strength and stiffness in hindwings but also play an important role for interlocking the action of crease lines. The deploying actions are caused by the skeletomuscular apparatus of the metathorax (8, 14) and are propagated to the wing apex direction by these thick veins. Therefore, ladybird beetles can interlock the movement of two transverse folding lines and achieve compact wing folding and quick deployment. *C. septempunctata* has a crease pattern similar to the crease pattern of the other ladybird *Aiolocaria* sp. reported by Fedorenko (8). According to Forbes (1), *Epilachna borealis* (Fabricius) and *Anatis 15-punctata* (Olivier) also possess similar crease patterns with the minor difference of additional small fold lines in the posterior margin. A diamond-shaped crease pattern similar to the green lines in Fig. 1*B* was also found in these ladybird beetles and can be regarded as an important feature of their hindwings. Fig. 3*A* shows the schematic of the folding movement of this pattern. Note that this figure shows the ventral side of the hindwing; therefore, the mountain and valley assignments of folding lines are exchanged from the case of Fig. 1*B*. These diamond-shaped crease lines have little involvement in the global deformation of the wings but cause the additional fold on the ridge of the central folding line, as indicated by the red circle in Fig. 3*A*. One possible function of this additional fold is the lock mechanism that helps avoid accidental unfolding caused by wing elasticity. Fig. 3*B* shows the semi-transparent image of the folded hindwing. As shown in the red circle in this figure, the additional fold of the diamond-shaped crease is fixed by tucking between the MCL and RML (also Movie S3). It can be considered that this tucking functions to maintain the folded shape in the PTF. An additional possible function may be to introduce bistability into the structure. The bistable behavior of the hindwings, which is considered to assist wing transformation and shape locking, has been reported in many previous studies (1–3, 6, 8); however, its detailed mechanisms remain unclear. Considering the structural stability, the crease pattern evident in Fig. 3*A* has a negative degree of freedom; hence, it is not rigidly foldable in general (15, 16) (*Rigid Foldability in Origami Crease Patterns*). Therefore, the act of folding and unfolding should be accompanied by elastic deformations. These deformations in nonrigid origami usually emerge as stretching and shrinkage of fold lines, fold line drifts, and out-of-plane deformation of facets. In the case of these diamond-shaped crease lines, out-of-plane deformations are considered

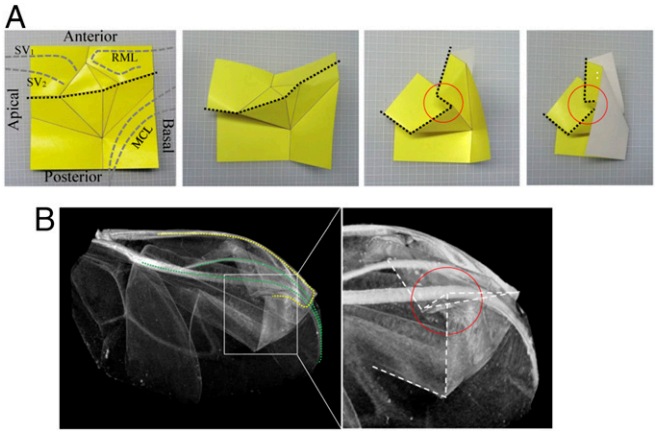

Fig. 3. Schematic of the folding movement in the wing central part (from the ventral side of the right hindwing). (*A*) Diamond-shaped crease lines, which are characteristic of hindwings in ladybird beetles, have little involvement in the global deformation of wings but cause the additional fold on the ridge of the central folding line, as indicated by the black dotted lines and red circles. (*B*) Translucent image of a folded hindwing in *C. septempunctata*. The additional fold part (white dotted lines) is positioned between the RML (yellow dotted line) and MCL (green dotted line) (also Movie S3).

the dominant factor. Observing the wing structure, the facets as presented in Fig. 3*A* are not wholly hard plates but are partially supported by veins; therefore, these facets can readily cause out-of-plane deformation involving some diagonal lines. In fact, it can be confirmed that certain facets in the paper model of Fig. 3*A* result in out-of-plane deformations during the folding process. This elastic deformation in the folding/unfolding process is considered to impart the bistable behavior to hindwings.

From an engineering standpoint, the most interesting aspect of hindwings in beetles is how they can achieve the compatibility between the deformability (or instability) required for the wing storage and the strength properties (or stability) required for flying. These two properties generally demonstrate a trade-off relationship, and thus are difficult to combine (*Crease Patterns and Supporting Structures in Beetle Hindwings*). Ladybird beetles have successfully resolved these two conflicting requirements, resulting in the evolution of relatively thick veins with decent strength properties while achieving sufficiently compact wing folding with two folding lines in the longitudinal direction of the wing. It is noteworthy that Fedorenko (17) concluded that ladybird beetles are categorized as one of the most advanced groups within the context of wing folding.

The biggest challenge for ladybird beetles is that they are required to embed the two transverse folding lines (PTF and ATF) on the anterior margin, which acts as the main support structure of the hindwing during flight. Simple articulations or positionally fixed compliant hinges in this area may cause a considerable decrease in the stiffness and strength of the wing. Our results show that ladybird beetles solve this problem by using tape spring-like veins as the main wing-supporting structures. A tape spring is a thin elastic strip with a curved cross-section that is commonly known as a carpenter tape. This structure becomes elastically stable when it is extended and can be stored into a compact form only by elastic folding (10); therefore, it is widely used in the extension booms and hinges of space-deployable structures (11–13). Fig. 4 presents a schematic of the functions of tape spring-like veins in wing folding/unfolding. These veins are stabilized in the unfolded shape and can confer sufficient stiffness for flight (Fig. 4*A*). Based on finite element analysis that was conducted on a simple shell model of the SV_2 vein obtained from the results of micro-CT scanning, this curved cross-section has about 11-fold greater bending stiffness than flat-shaped veins of the same weight (*Finite Element Analysis of the Tape Spring-Like Vein* and Fig. S3). If the specific stiffness is the only issue, more effective forms were found in insect wings. For example, wing veins in the dragonfly have a tubular sandwich microstructure (18). It is also reported that the elytra of beetles are constructed with honeycomb-like sandwich structures (19). Besides the structural reinforcement property, tape spring veins have three unique properties enabling wing folding/unfolding in ladybird beetles. First, the veins can be bent at an arbitrary position by forming localized folds during wing storage, and therefore can serve as compliant hinges where appropriate. As shown in Fig. 1 *D* and *E*, the edge of the elytron is used to initialize this folding (Fig. 4*B*). A second characteristic of this structure is its ease of moving the bending point (position of the localized fold) along the beam length (Fig. 4*C*). The revealed folding processes include the drift of the ATF in the basal-to-apex direction as shown in Fig. 1*F*. This drifting fold is considered to enable gradual wing retractions. The third function of the tape spring vein is to store elastic energy for wing deployment (Fig. 4 *D* and *E*). The elastic force caused by the resilience in the localized folds is considered to enable rapid wing deployments in ladybird beetles (Movie S1). With respect to wing-deploying forces, it is reported that some beetles use hydraulic mechanisms that may straighten the hindwings by blood pressure (7). Our micro-CT investigation shows no concrete evidence regarding whether ladybird beetles exhibit similar mechanisms (e.g., cavities in hindwings, inflation of unfolded veins). Further investigations, particularly of the cross-sections of wing veins, by scanning electron microscopy (SEM) and microtome are warranted to clarify this issue.

The detailed wing-folding mechanism revealed in the present study is expected to facilitate understanding of the optimization process that has developed during the course of evolution, which can elucidate the innovative design method enabling the integration of both structural stability and deformability. Immediate applications may be deployable structures, including space-deployable structures represented by solar array paddles and antenna reflectors of satellites, wings of carrier-based aircrafts, and many articles of daily use with a deforming function (e.g., umbrellas, fans). The relationship between the wing-actuating mechanisms and latest mechanics is similarly interesting. The deformations include elastic behavior in the supports, and therefore can be determined as the compliant mechanism (20, 21). This mechanism is an active research target within the mechanics and microelectromechanical system fields. In regard to the geometry of the crease pattern, Brackenbury (3) and Haas and Wootton (22) proposed a simplified geometrical model based on the characteristic patterns found in most beetles. These studies have recently been considered to gain importance because of the advancement in applied origami (23–27). Combined with these emerging technologies, the wings of beetles will have a great impact on multiscaled production in various engineering fields.

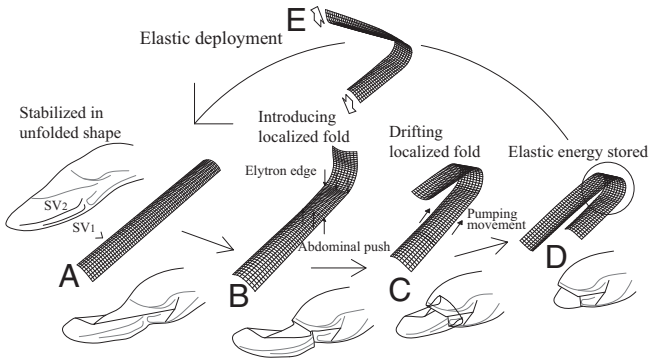

Fig. 4. Schematic of the functions of tape spring-like veins. (*A*) Veins are stabilized in the unfolded position and able to confer sufficient stiffness for flight. (*B*) Veins can be bent at an arbitrary position by forming localized folds during wing storage. The edge of the elytron is used to initialize this folding. (*C*) It is easy to move the bending point (position of the localized fold) along the beam length in tape spring veins. (*D* and *E*) Storing elastic energy for wing deployment. The elastic force caused by the resilience of the localized folds is considered to enable rapid wing deployments in ladybird beetles.

Materials and Methods

Transplant Operation. Specimens used were of the ladybird beetle species *C. septempunctata* (L.) (Coleoptera: Coccinellidae) and were captured in the grass fields of Tokyo, Japan. Each specimen was anesthetized using carbon dioxide gas, and two-thirds of its right apical elytron was excised using scissors. Silicone (Sildefit wash-XS; SHOFU Co., Ltd.) was used to construct the impression of the undersurface of the excised elytron. The curing time was 5 min at 25 °C. The UV-cured resin (Craft arrange clear; CHEMITECH, Inc.) was applied in a thin layer on the impressions using a brush. After curing by UV light, the transparent acrylic elytron was fabricated. These artificial wings were adhered on the apices of the excised wings of the original ladybird beetles using a UV-cured resin. Each transplant operation was completed in ≤1 h to minimize the damage to the hindwings and living beetles.

Observations by High-Speed Cameras. The specimens were placed on an acrylic board and were kept in focus by simultaneously moving the board on the table to maintain their position in the frame. High-speed cameras (Phantom V1611, Nobby Tech. Ltd.; VW9000, KEYENCE CORPORATION; and HAS-L2, DITECT Co., Ltd.) were used to acquire slow-motion movies. The

wing-deploying scenes (Movie S1) were filmed using 3,000 and 4,000 frames per second (fps), whereas the folding scenes (Movie S2) used 60 fps.

Micro-CT. This study used the microfocus X-ray CT system, inspeXio SMX-100CT (SHIMADZU CORPORATION), which comprises a nonenclosure tube-type X-ray generator operating at a voltage of 100 kV. Specimens used were the folded and unfolded hindwings of *C. septempunctata* vertically mounted on the stage along the wing-length direction. CT images were acquired for each 10-μm length at a resolution of 1,024 × 1,024 pixels and reconstructed into 3D images using the visualization software VGStudio MAX (Volume Graphics GmbH).

ACKNOWLEDGMENTS. We thank M. Maruyama for meaningful discussions during the early days of the study, F. Tomoike for giving useful advice about manufacturing of the artificial wings, A. Igarashi for supporting the capture and upkeep of the ladybird beetles, and Nobby Tech. Ltd. and KEYENCE CORPORATION for providing high-speed cameras. This work was supported by the Special Fund of the Institute of Industrial Science, the University of Tokyo; Japan Society for the Promotion of Science, Grants-in-Aid for Scientific Research (KAKENHI) Grants 24860024 and 17H04911; Asahi Glass Foundation Research Encouragement grants (2016); and Japan Science and Technology Agency, Exploratory Research for Advanced Technology (ERATO) Grant JPMJER1501. The work of S.N. is supported, in part, by KAKENHI Grant 24120002.

1. Forbes WTM (1926) The wing folding pattern of the Coleoptera. *J NY Entomol Soc* 24: 91–139.
2. Hammond PM (1979) Wing-folding mechanisms of beetles, with special reference to investigations of adephagan phylogeny (Coleoptera). *Carabid Beetles, Their Evolution, Natural History, and Classification*, eds Erwin TL, Ball GE, Whitehead DR (Dr W. Junk, The Hague), pp 113–180.
3. Brackenbury JH (1944) Wing folding and free-flight kinematics in Coleoptera (Insecta): A comparative study. *J Zool* 232:253–283.
4. Schneider VP (1978) Flight types and hinding folding in Coleoptera. *Zool Jahrb Abt Anat Ontogenie Tiere* 99:174–210.
5. Saito K, Yamamoto S, Maruyama M, Okabe Y (2014) Asymmetric hindwing foldings in rove beetles. *Proc Natl Acad Sci USA* 111:16349–16352.
6. Haas F, Gorb S, Blickhan R (2000) The function of resilin in beetle wings. *Proc Biol Sci* 267:1375–1381.
7. Sun J, Ling M, Wu W, Bhushan B, Tong J (2014) The hydraulic mechanism of the unfolding of hind wings in *Dorcus titanus platymelus* (order: Coleoptera). *Int J Mol Sci* 15:6009–6018.
8. Fedorenko DN (2009) *Evolution of the Beetle Hind Wing, with Special Reference to Folding (Insects, Coleoptera)* (Pensoft Publishers, Sofia, Bulgaria).
9. Kukalová-Peck J, Lawrence JF (1993) Evolution of the hind wing in Coleoptera. *Can Entomol* 125:181–258.
10. Seffen KA, Pellegrino S (1999) Deployment dynamics of tape springs. *Proc R Soc A* 455: 1003–1048.
11. Mobrem M, Adams D (2009) Deployment analysis of lenticular jointed antennas onboard the Mars express spacecraft. *J Spacecr Rockets* 46:394–402.
12. Mallikarachchi HMYC, Pellegrino S (2009) Deployment dynamics of ultrathin composite booms with tape-spring hinges. *J Spacecr Rockets* 51:604–613.
13. Kwok K, Pellegrino S (2013) Folding, stowage, and deployment of viscoelastic tape springs. *AIAA Stud J* 51:1908–1918.
14. Haas F, Beutel RG (2001) Wing folding and the functional morphology of the wing base in Coleoptera. *Zoology (Jena)* 104:123–141.
15. Watanabe N, Kawaguchi K (2009) The method for judging rigid foldability. *Origami4*, ed Lang JR (A K Peters, Natick, MA), pp 165–174.
16. Tachi T (2010) Geometric considerations for the design of rigid origami structures. Proceedings of the International Association for Shell and Spatial Structures Symposium, eds Zhang Q, Yang L, Hu Y, (China Architecture & Building Press, Beijing), pp 771–782.
17. Fedorenko DN (2015) Transverse folding and evolution of the hind wings in beetles (Insecta, Coleoptera). *Biol Bull Rev* 5:71–84.
18. Ren H, Wang X, Li X, Chen Y (2013) Effects of Dragonfly wing structure on the dynamic performances. *J Bionic Eng* 10:28–38.
19. Chen J, Xie J, Wu Z, Elbashiry EMA, Lu Y (2015) Review of beetle forewing structures and their biomimetic applications in China: (I) On the structural colors and the vertical and horizontal cross-sectional structures. *Mater Sci Eng C* 55:605–619.
20. Howell LL (2001) *Compliant Mechanisms* (Wiley–Interscience, New York).
21. Smith ST (2000) *Flexures: Elements of Elastic Mechanisms* (CRC Press, Boca Raton, FL).
22. Haas F, Wootton RJ (1996) Two basic mechanisms in insect wing folding. *Proc R Soc Lond B Biol Sci* 263:1651–1658.
23. Saito K, Tsukahara A, Okabe Y (2016) Designing of self-deploying origami structures using geometrically misaligned crease patterns. *Proc R Soc A* 472:20150235.
24. Saito K, Tsukahara A, Okabe Y (2015) New deployable structures based on an elastic origami model. *J Mech Des N Y* 137:021402.
25. Felton S, Tolley M, Demaine E, Rus D, Wood R (2014) Applied origami. A method for building self-folding machines. *Science* 345:644–646.
26. Filipov ET, Tachi T, Paulino GH (2015) Origami tubes assembled into stiff, yet reconfigurable structures and metamaterials. *Proc Natl Acad Sci USA* 112:12321–12326.
27. Chen Y, Peng R, You Z (2015) Applied origami. Origami of thick panels. *Science* 349: 396–400.
28. Shi NN, et al. (2015) Thermal physiology. Keeping cool: Enhanced optical reflection and radiative heat dissipation in Saharan silver ants. *Science* 349:298–301.
29. Burrows M, Sutton G (2013) Interacting gears synchronize propulsive leg movements in a jumping insect. *Science* 341:1254–1256.
30. Gao X, Jiang L (2004) Biophysics: Water-repellent legs of water striders. *Nature* 432: 36.
31. Gorb SN (1998) Frictional surfaces of the elytra-to-body arresting mechanism in tenebrionid Beetles (Coleoptera tenebrionidae): Design of co-opted fields of microtrichia and cuticle ultrastructure. *Int J Insect Morphol Embryol* 27:205–225.
32. Belcasro SM, Hull TC (2002) Modelling the folding of paper into three dimensions using affine transformations. *Linear Algebra Appl* 348:273–282.
33. Tachi T (2009) Simulation of rigid origami. *Origami4*, ed Lang JR (A K Peters, Natick, MA), pp 175–187.
34. Thompson DW (1917) *On Growth and Form* (Cambridge Univ Press, Cambridge, UK).
35. Vincent JFV, Wegst UGK (2004) Design and mechanical properties of insect cuticle. *Arthropod Struct Dev* 33:187–199.
36. Takaku Y, et al. (2013) A thin polymer membrane, nano-suit, enhancing survival across the continuum between air and high vacuum. *Proc Natl Acad Sci USA* 110: 7631–7635.

Supporting Information

Saito et al. 10.1073/pnas.1620612114

Assisting Structures for Wing Folding

SEM observations identified various microdevices in the body of insects, which confer versatile functions (28–31). Previous studies reported the existence of the microspicules and trichia on the abdominal terga, underside of the elytra, and surface of hindwings in various species of beetles (2, 4). These microstructures are believed to fulfill functions for the elytra/abdomen in interlocking in the resting position and supporting wing folding. In the beetles with complex foldable hindwings, represented by rove beetles (Staphylinidae) and ladybird beetles, the patch-like structures dense with microspicules are commonly observed on the tergites, known as wing-folding spicule patches (2). Fig. S2 shows the abdominal tergite and wing-folding spicule patches in *Coccinella septempunctata*. These patches are positioned on tergites 2–6. Each plate contains a pair of patches in the median region, and tergites 5 and 6 contain additional patches laterally. Tergite 7 appears to contain no patch-like structures but is instead uniformly covered by smaller spicules. It is evident that the positions of these patches are related to the resting position of the hindwings. The spicule directions of the patches on tergites 4–6 that are positioned just under the folded hindwings have complex patterns. The patches are considered to fulfill functions to increase (or decrease) friction for a particular direction on the abdominal terga and to bind wing membranes in the proper position in midfolded shapes. By the presence of these wing-folding spicule patches, simple up-and-down movements of the abdomen can achieve the complex folding patterns with two transverse folding lines. In regard to the undersurface of the elytra, our SEM observations identified no observable microstructures, except for the microspicules in the center of the basal position and lateral side. Considering the position of these spicules, they are believed to be the elytra interlocking structures (31) and probably have no function for supporting wing folding.

Rigid Foldability in Origami Crease Patterns

Rigid foldability (15, 16) is an important property in origami crease patterns. If the given crease pattern is rigid-foldable, it means that the facets and fold lines can be replaced with rigid panels and ideal hinges, respectively, and the origami pattern can be folded without facet deformations. Under rigid-foldable conditions where origami can be described by geometric restrictions, researchers have proposed several methods for simulating the folding process (32, 33). The rigid foldability of a given crease pattern can be investigated by the mechanical degree of freedom (DOF). If the crease pattern has no hole and there is no redundant constraint, the DOF is expressed by the following equation (16):

$$\mathrm{DOF} = N_{\mathrm{E}} - 3N_{\mathrm{V}}, \qquad \textbf{[S1]}$$

where N_{E} is the total number of fold lines and N_{V} is the total number of vertices. When DOF ≥ 1, the crease pattern is determined to be rigid-foldable. Fig. 3*A* has 14 folding lines and five vertices; thus, the DOF is calculated as −1. Therefore, this pattern is not rigidly foldable in general, and its folding/unfolding process should include the elastic deformations of facets.

Crease Patterns and Supporting Structures in Beetle Hindwings

Although beetles show enormous diversity in body size and shape and there are large differences in the crease patterns and shapes of the supporting structures in hindwings among species, it is possible to discuss the following general tendency (1, 8, 9, 34). Large-sized beetles, such as rhinoceros and other scarab beetles (Scarabaeidae), require intense wing flapping to gain the lifting force to counterbalance their heavy weight; therefore, they have generally developed thick veins that confer high rigidity and strength in wings. The wing-folding mechanisms in these types of beetles are inevitably simple and, in most cases, use a single folding along the longitudinal direction (1, 8). Additional small transverse folding lines are found in the wing apexes of some of these beetles; however, they separate the movements of the main folding lines and do not contribute to the storing efficiency. On the other hand, small-sized beetles, such as ant-loving beetles (Staphylinidae: Pselaphinae), require little rigidity in hindwings and have relatively thin veins with sufficient flexibility, which are beneficial for compact wing folding. For example, some species of ant-loving beetles fold the hindwings using accordion-like patterns with six or seven transverse folding lines (1). Some groups of rove beetles fold the hindwings using right-to-left asymmetrical crease patterns, thereby achieving highly compact wing folding (5). From a standpoint of engineering applications, the high rigidity and strength of wings in large-sized beetles are attractive; however, the storing efficiency is not high. The highly compact wing folding found in small-sized beetles is very interesting; however, the weakness in the mechanical properties of the wings limits the possible applications. Ladybird beetles are believed to occupy an intermediate position between these two groups.

Finite Element Analysis of the Tape Spring-Like Vein

To demonstrate the structurally reinforcing properties of the tape-spring vein, the commercial finite element analysis (FEA) software ANSYS was used to simulate the static bending test. The finite element model was made from the surface data of SV_2, which was extracted from the results of micro-CT scanning (Fig. 2*A*). A total of 5,809 shell elements were used to model the SV_2 vein. Per the micro-CT results, the cell thickness was set to 0.015 mm, approximately the average thickness of the vein. The cuticle, the main material for hindwings, is known to exhibit a very wide range of mechanical properties depending on the citin fiber and moisture content (35). It is difficult to measure Yong's module of the vein cuticle from a living ladybird beetle. This study used Yong's module of the general wing cuticle (6.0 GPa), as described by Vincent and Wegst (35). For simplified discussion, the isotropic linear elastic element was used. The basal edge line of the numerical model was completely fixed, and 5.0×10^{-4} N of a uniformly distributed load (nearly equal to the weight of a ladybird beetle) was applied on the top surface in the vertical direction (−Z in Fig. S3). For comparison, the same flat-shaped plate with an equal weight was simulated using the same material and boundary conditions. Fig. S3 shows the calculated result. Maximum displacements are 0.068 mm (tape spring) and 0.7 mm (flat plate); therefore, the tape spring cross-section has about 11-fold higher bending stiffness than the flat-shaped vein. With respect to the strength of cuticle, there are data reporting that the tensile strength of a locust femoral cuticle is 60–200 MPa, which is about 1–5% of the stiffness (35). According to the FEA result, the maximum stress of the tape spring model is 15.2 MPa (about 0.5% of the stiffness). Therefore, it can be said that the tape spring vein possesses sufficient strength to withstand the same level of the static load as the body weight. Actual wing veins are not uniform solid plates but have complex inner structures, and their material composition also exhibits anisotropic and nonlinearity properties. Therefore, the above value should only be used as a reference. Although further experimental investigation is required to determine accurate mechanical properties of the hindwings, these results show that tape spring veins have large structural reinforcement properties.

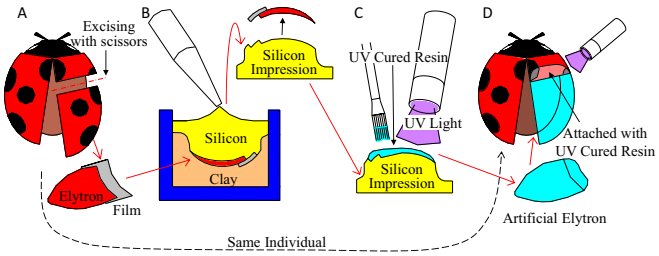

Fig. S1. Schematic representation of the transplant operation. (*A*) Ladybird beetle was anesthetized using carbon dioxide gas, and two-thirds of its apical right elytron was excised using scissors. To construct the connecting portion, a small-sized thin film was attached on the top surface of the cut plane on the excised elytron. (*B*) Elytron and film are mounted on the clay with the ventral surface up, and two-part silicone (Sildefit wash-XS; SHOFU Co., Ltd.) was applied. After curing (5 min at 25 °C), the elytron and film were peeled off from the impression. (*C*) UV-cured resin (Craft arrange clear; CHEMITECH, Inc.) was applied in a thin layer on the impressions using a brush. After curing by UV light, the transparent acrylic elytron was fabricated. (*D*) Artificial elytron was adhered to the apices of the right wing of the original ladybird beetles using the UV-cured resin.

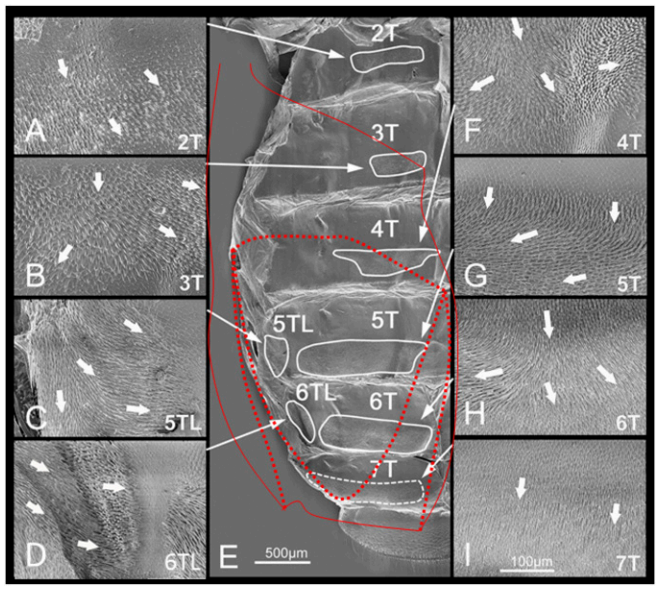

Fig. S2. Abdominal tergites and wing-folding spicule patches in *C. septempunctata*. These figures were micrographed using SEM. (*A–D* and *F–I*) Wing-folding spicule patches. (Magnification: 1,000×.) (*E*) Abdominal tergites. (Magnification: 200×.) The red dotted lines show the position of the folded hindwing in a resting state. 2T to 7T, abdominal tergites 2–7; 5TL and 6TL, abdominal tergites 5 and 6, lateral patch. The white arrows show the directions of the spicules. The SEM sample was dissected from the insect specimen, uncoated, and treated using the nanosuits method (36). The sample was observed and photographed using a digital microscope system (KEYENCE VHX-2000 + VHX-D510) under an accelerating voltage of 1.2 kV.

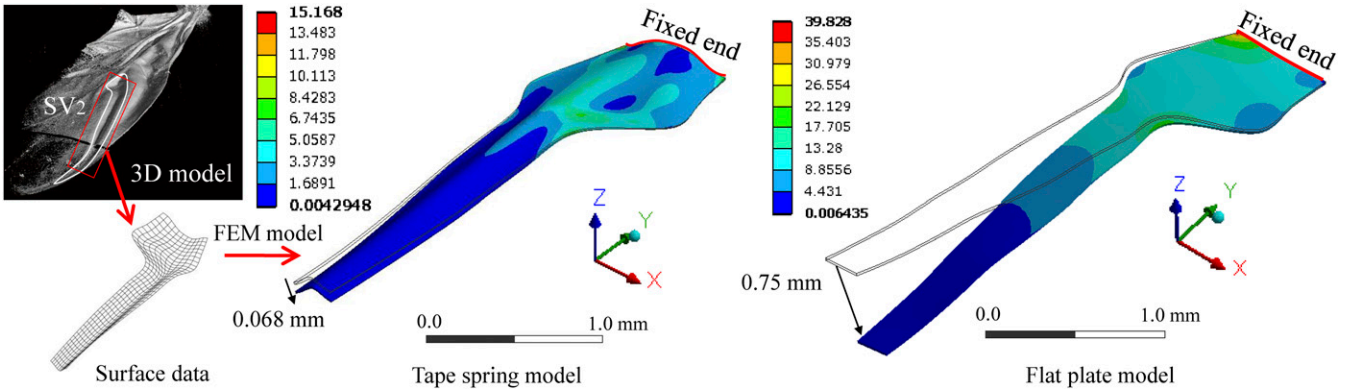

Fig. S3. Simulated results of the bending test in the tape spring vein. Commercial finite element analysis software, ANSYS, was used to simulate the static bending test. (*Left* and *Center*) Tape spring model was made from the surface data of SV_2, which was extracted from the results of the micro-CT scans. A total of 5,809 shell elements were used to model the SV_2 vein. For comparison, the flat plate model (5,105 shell elements) was made from the side edges of the tape spring model (*Right*). The isotropic linear elastic element (Yong's module = 6.0 GPa, Poisson's ratio = 0.3) was used in both models. Basal edge lines of the numerical models were completely fixed, and a 5.0×10^{-4} N uniformly distributed load (almost equal to the weight of a ladybird beetle) was applied on the top surface along the $-z$ axis. The color bars illustrate the equivalent stress (measured in megapascals).

Movie S1. Wing-deploying motion of a ladybird beetle imaged with a high-speed camera. The hindwing deployment in the takeoff motion was very fast and completed within 0.1 s from the fully folded state.

Movie S1

Movie S2. Wing-folding motion of a ladybird beetle imaged with a high-speed camera. Ladybird beetles are known to use their elytra and abdomen for folding. The transplantation of the artificial acrylic elytron enables a detailed observation of these wing-folding techniques.

Movie S2

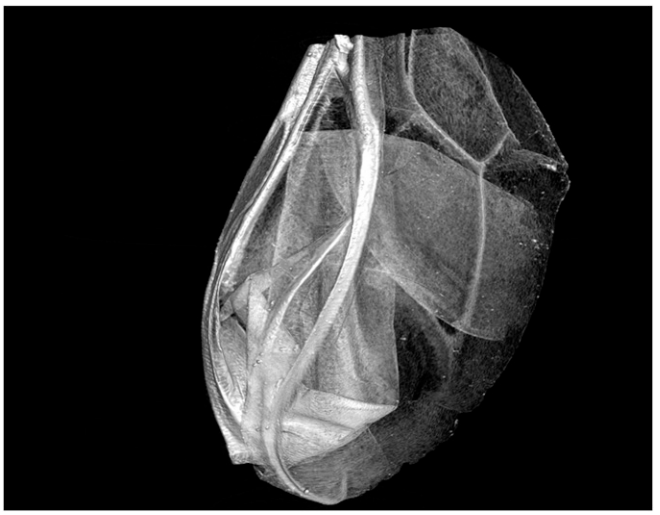

Movie S3. Translucent image of the folded hindwing in *C. septempunctata* reconstructed by the result of the micro-CT scan. The wing is not folded into a flattened shape but has slightly open angles to fit into the storage space between the elytron and abdomen.

Movie S3